The largest instrumentally recorded earthquake in Taiwan: revised location and magnitude, and tectonic significance of the 1920 event

T. Theunissen, Y. Font, S. Lallemand, W.T. Liang

Geophysical Journal International

Geophys. J. Int. (2010) **183,** 1119–1133 doi: 10.1111/j.1365-246X.2010.04813.x

The largest instrumentally recorded earthquake in Taiwan: revised location and magnitude, and tectonic significance of the 1920 event

Thomas Theunissen,[1] Yvonne Font,[2] Serge Lallemand[1,3] and Wen-Tzong Liang[4]

[1] *Geosciences Montpellier, UMR* 5243, *CNRS, University of Montpellier* 2, *France. E-mail: theuniss@gm.univ-montp2.fr*
[2] *Geoazur, UNS-IRD-OCA, Villefranche-Sur-Mer, France*
[3] *LIA (Associated International Laboratory) ADEPT (Active Deformation and Environment Programme for Taiwan), Taiwan and France*
[4] *Institute of Earth Sciences, Academia Sinica, Taipei, Taiwan*

Accepted 2010 September 16. Received 2010 September 3; in original form 2010 March 16

SUMMARY

The Ryukyu subduction is known to generate very few earthquakes in its central segment contrarily to its two extremities. We focus in this study on the southernmost part of the Ryukyu subduction zone offshore east Taiwan. Our first task was to build a homogeneous earthquake catalogue for the period 1900–2007. The new catalogue provides homogenized M'_W magnitudes and shows that several $M'_W \geq 7.0$ earthquakes occurred offshore Hualien and Suao cities. We then focused on the 1920 June 5 earthquake (reported surface wave magnitude 8.1) previously located beneath the accretionary prism. The revised moment magnitude has been estimated in our catalogue at 7.7 ± 0.2. It is the biggest earthquake ever recorded in the Taiwan area but the fault that has produced this earthquake has not yet been identified with confidence. We relocated this event using regional phases (seismological bulletins archived at the Central Weather Bureau of Taiwan) about 50 km NNE and shallower of its former location, that is, within the Ryukyu Arc basement. According to earthquake bulletin information, revised magnitude, new hypocentral determination and known regional faults, we propose four potential active faults as candidates for the slip associated to this event: (1) the interplate seismogenic zone (ISZ), (2) an out-of-sequence thrust cutting through the forearc and branching on the ISZ, (3) a NS strike-slip fault cutting through the Ryukyu arc and (4) a N–S, westward dipping thrust fault, affecting the Philippine Sea Plate east of the Luzon Arc. The best compromise is to consider a rupture along the ISZ with a shallow nucleation possibly along a splay-fault followed by a downward and lateral propagation of the rupture that would explain the lack of significant seafloor motion and subsequent tsunami. We also estimate the maximum seismic coupling of the ISZ in the region east of Taiwan to about 0.4. In parallel, the evidences of aseismic slip occurring along the ISZ allow us to conclude that this region should only be affected by $M <$ 8 earthquakes.

Key words: Seismicity and tectonics; Subduction zone processes; Continental margins: convergent; Dynamics: seismotectonics.

1 INTRODUCTION

Taiwan is one of the most tectonically active regions in the world. It is located in the transfer zone between two opposite verging subductions (Tsai *et al.* 1977; Wu 1978). South of the island, the Eurasian Plate (EP) is subducting eastwards under the Philippine Sea Plate (PSP), whereas east of Taiwan, the PSP is subducting northwards under the EP along the Ryukyu Trench. The Ryukyu subduction is associated with the backarc rifting of the Okinawa trough (Letouzey & Kimura 1986; Sibuet *et al.* 1986). Considering the EP fixed, the PSP converges northwestwards (∼312°N) at a rate of 8.1 cm yr^{-1} (Yu *et al.* 1997). Taiwan results from the collision between the passive continental margin of the South China Sea and the Luzon Volcanic Arc associated with the Manila Subduction (Biq 1972; Chai 1972; Malavieille *et al.* 2002) (Fig. 1). The subsequent deformation is characterized by a very high rate of seismicity onland, but also offshore east Taiwan (Hsu 1961; Wu 1978; Tsai 1986; Kao *et al.* 1998; Wang & Shin 1998; Wang 1998; Chen *et al.* 2009). The first permanent seismometer was installed in Taipei in 1897 and then the number of stations increased, reaching nowadays more than hundred stations. Therefore, from the beginning of the last century, ground motion in Taiwan has been continuously recorded with seismological networks evolving through time (Cheng & Yeh 1989; Wang 1998; Wang & Shin 1998). Various seismicity catalogues are

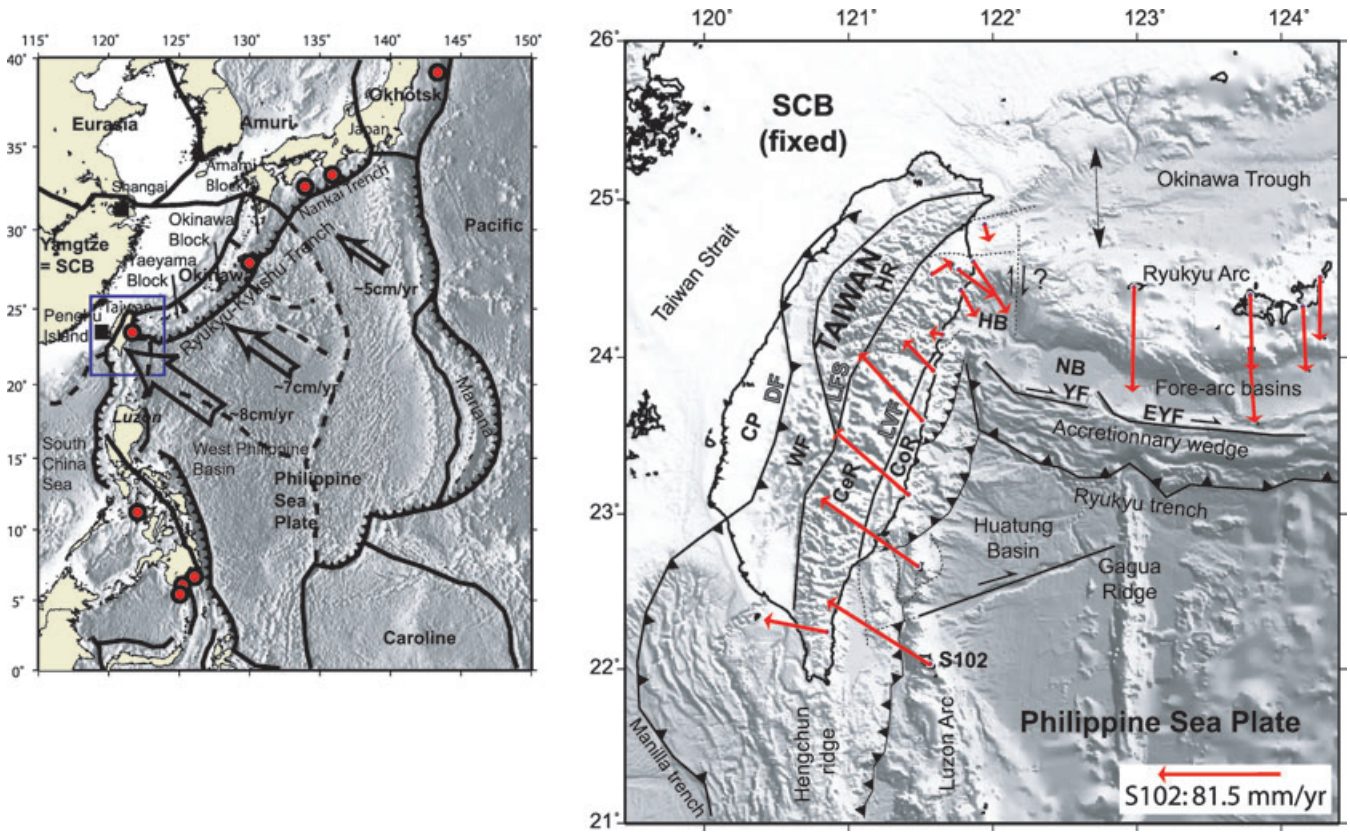

Figure 1. General tectonic context of the southernmost part of the Ryukyu subduction east of Taiwan. Left: contour of the Philippine Sea Plate (PSP) according to the global model of plate boundaries of Bird (2003) and relief from ETOPO1 (Amante & Eakins 2009). Large earthquakes with magnitude higher than eight are represented by red circles. Right: zoom on Taiwan area. Velocity of the PSP is given according to Penghu Island (Yu *et al.* 1997), that is, the South China Block (SCB) = ∼Eurasian Plate, and the velocity of the Ryukyu Arc is given according to the Shanghai VLBI station (Nakamura 2004), that is, also the SCB. DF: deformation front, CP: Coastal Plain (foreland), WF: Western-Foothills region, HR: Hsuehshan Range, LFS: Lishan Fault System, LVF: Longitudinal Valley faults System, CeR: Central Range, CoR: Coastal Range, HB: Hoping Basin, NB: Nanao Basin, (E)YF: (East) Yaeyama Fault.

available from 1900 to present (Lee *et al.* 1978; Hsu 1980; Cheng & Yeh 1989; Wang & Kuo 1995; Yeh *et al.* 1995; Chen & Tsai 2008; Chen *et al.* 2009). A review study of earthquakes (period 1897–1996) has been published in 1998 by Jeen-Hwa Wang. The 1999 September 21, M 7.6 so-called 'Chi-Chi' earthquake occurred in a densely populated region and caused about 2470 deaths, 11 305 injured and more than 100 000 structures destroyed (Shin & Teng 2001). It was undoubtedly the most devastating earthquake of the last century but it was not reported as the highest in magnitude. The greatest reported earthquake is supposed to have occurred on 1920 June 5 offshore Hualien, east of Taiwan (Fig. 2). Its surface wave magnitude has been estimated at 8.1 by Wang & Kuo (1995). The seismological bulletin shows that this earthquake is responsible for eight deaths, 24 injured and some building destruction 'but less than Puli earthquake in 1917' (M_L 6.0, but onland 50 km western Hualien). The most damaged areas were Taipei, Taoyuan, Hsinchu and Taitung coinciding with the most populated areas.

Kao (1998) and Shyu *et al*. (2005) have proposed that such a M 8 earthquake could have been generated along the Ryukyu Interplate Seismogenic Zone (ISZ), whereas Chung *et al.* proposed that it may have been associated with the northern part of the Longitudinal Valley Fault (LVF) (Chung *et al.* 2008). However, the 1920 earthquake has been located beneath the sedimentary accretionary prism (Cheng & Yeh 1989; Engdahl & Villaseñor 2002), seaward of the ISZ updip limit. Moreover, its depth is poorly constrained but is known to be shallow between 20 km (Cheng & Yeh 1989) and 35 km (Engdahl, van der Hilst and Buland (EHB) location) (Engdahl *et al.* 1998; Engdahl & Villaseñor 2002). None of the two initial candidate faults, that is, the ISZ and the LVF, coincide with the hypocentre determination. Several other seismically active faults have been identified in this region so the identification of the fault ruptured in 1920 is consequently debatable. We thus aim in this paper to improve the location of this major event, the biggest of the last century in the Taiwan area, to better constrain which fault has produced it.

1.1 Active faults

A number of active faults have been recognized or suspected east of Taiwan. Besides the LVF and the ISZ, other faults characterize the southernmost part of the Ryukyu subduction. The ISZ has been described by Kao *et al.* (1998) and Kao (1998) using the inversion of teleseismic data to determine source parameters. They concluded that the ISZ is not strongly coupled and that the apparent slip partitioning indicates that the Ryukyu forearc is not completely elastic and thus the ISZ is unlikely to generate $M_W >$ 8 subduction earthquakes. Otherwise, Hsu (2001) concluded that the ISZ is potentially coupled according to the flat curve section of the mantle lithospheric buoyancy across the Ryukyu margin. Regarding the LVF, the shallow northern part is characterized by a smaller convergence rate north of 23.5°N than in the south and an important left-lateral movement along a thrust dipping eastwards.

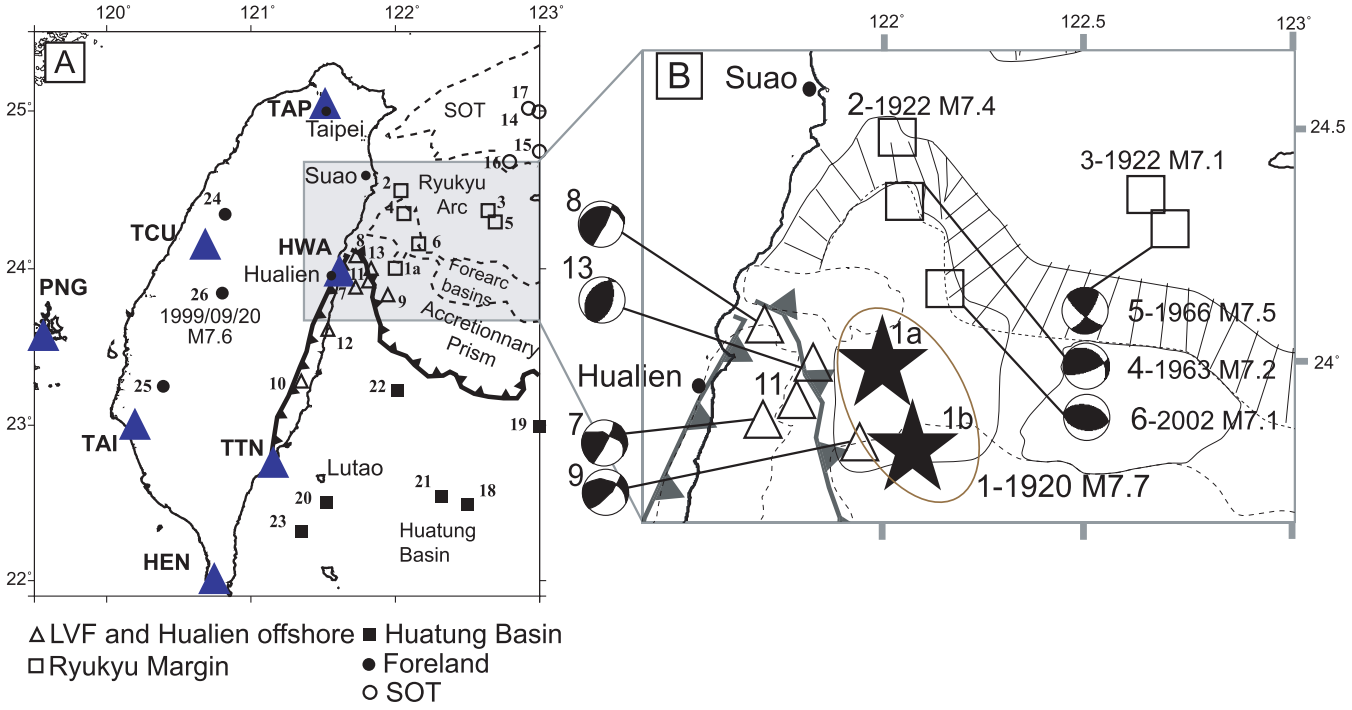

Figure 2. Earthquakes with equivalent moment magnitudes $M'_W \geq 7.0$ (see Table S1 in the Supporting Information for references about all earthquakes). (A) Triangle: available seismic stations during the 1920 earthquakes. (B) Close-up view of the Ryukyu margin with the two locations for the 1920 earthquake proposed in the literature: '1a' after TMO [Taihoku (Taipei) Meteorological Observatory], depth 20 km, and '1b' after the centennial catalogue (Engdahl & Villaseñor 2002) obtained with the EHB process (Engdahl *et al.* 1998) depth 35 km. Focal mechanisms source: 4: (Chen *et al.* 2004); 5:13: (Kao *et al.* 1998); 6: BATS; 7,8,9: (Cheng *et al.* 1996). SOT: Southern Okinawa Trough.

The east-dipping deeper part of the LVF extends offshore (Kuochen *et al.* 2004; Shyu *et al.* 2005; Chung *et al.* 2008). Some authors have also suggested that the PSP itself was deforming. Buckling of the PSP slab in response to the E–W compression generated by the collision has been demonstrated (Font *et al.* 1999; Wang *et al.* 2004; Wang 2005; Chou *et al.* 2006) and may cause important seismic deformation. Chemenda *et al.* (1997, 2001), based on physical modelling, have suggested that an incipient westward dipping subduction could develop offshore east of Hualien. Later, Font (2002) and Bos *et al.* (2003) have found some evidences of such intra-PSP N–S reverse fault trending N–S and east of the Luzon arc beneath the Ryukyu forearc. Regarding the deformation of the Ryukyu upper plate, careful examination of the seismicity distribution supports the hypothesis of a possible splay fault, or even high-angle backthrust cutting through the forearc along the Hoping canyon (Font & Lallemand 2009). Furthermore, important N–S strike-slip faults could affect the Ryukyu arc and forearc (Wu 1978; Lallemand & Liu 1998). West of the Hoping canyon, a N–S strike-slip fault zone offsetting the Ryukyu arc in response to the opening of the Okinawa backarc basin has been proposed by Lallemand & Liu (1998). As a matter of fact, southwest Ryukyu subduction termination does not show classical characteristics due to its recent and past collision history (Lallemand *et al.* 2001; Malavieille *et al.* 2002; Sibuet & Hsu 2004).

1.2 Historical earthquakes studies

The area east of Taiwan is unfortunately characterized by a poor azimuthal coverage either by the Taiwanese seismological network or the Japanese one, so that regional studies of historical instrumental earthquakes are not accurate. Kao *et al.* (1998), using teleseismic data to inverse source parameters for 62 moderate earthquakes ($M > 5.5$) between 1966 and 1995, have characterized the seismo-tectonic picture of this area including the ISZ. The centroid moment tensor (CMT) catalogue has been completed for shallow earthquakes in Taiwan area ($M > 6$) for the 1963–1975 period (Chen *et al.* 2004) in agreement with focal mechanisms determined previously (Katsumata & Sykes 1969; Wu 1970; Wu 1978; Pezzopane & Wesnousky 1989). Before 1962, other works focus on some seismic crises, like those of 1951 (Fig. 2) that occurred along the LVF, associated with important civil and building damages (Chen *et al.* 2008; Chung *et al.* 2008; Lee *et al.* 2008). However, several major earthquakes, which occurred offshore, have not yet been studied. It is thus crucial to improve our knowledge about the characteristics of these earthquakes to better constrain seismic hazard and tectonic processes in this area.

In this study, we focus on the biggest earthquake ever recorded in the Taiwan area: the *M*s 8.1 1920 shallow earthquake (Wang & Kuo 1995) that occurred offshore, about 50 km east of Hualien (Fig. 2). The location given in the centennial catalogue (EHB location) (Engdahl *et al.* 1998; Engdahl & Villaseñor 2002) as well as those from archives (Cheng & Yeh 1989) are ambiguous since it is difficult to associate this major earthquake to a known active fault. Also, an adapted revised moment magnitude is necessary to better constrain the size of the surface rupture.

2 RE-EVALUATION OF THE MOMENT MAGNITUDE

To better describe this event, our first task was to build a homogeneous seismicity catalogue by computing a homogenized moment magnitude despite the heterogeneity of the seismological network

used through time. Discussions and references on Taiwan Seismological Network evolution can be found in the works of Wang (1998), Wang & Shin (1998), Chen & Tsai (2008) and Ng *et al.* (2009). We only give a brief summary of the evolution of the seismological network in Taiwan.

Three stages of instrumental seismic observations by the Taiwanese Seismological Network can be identified: (1) 1897–1972: the period (0–16 stations) where only mechanical seismographs were used. Before 1945, the studies of numerous disastrous earthquakes and field surveys of the related damages were mainly done by Japanese seismologists, geologists and engineers of the TMO [Taihoku (Taipei) Meteorological Observatory]. First, seismographs were installed in Taipei (1897), Tainan (1898), Keelung (1900–1916), Penghu (1900), Taichung (1902), Hengchun (1907), Taitung (1903) and Hualien (1914) (Cheng & Yeh 1989). For all stations, the seismograms were recorded in an analogue form. (2) 1973–1991 TTSN (Taiwan Telemetered Seismological Network) (up to 24 stations) (3) 1991–present CWBSN (Central Weather Bureau Seismological Network) and BATS (Broadband Array in Taiwan for Seismology, 1995–present) (up to about 100 stations).

2.1 Building of a 1900–2007 seismicity catalogue of the Taiwan area

Over the Taiwan area (21°N–26°N and 119°E–123°E), we have used a compilation of different catalogues: the centennial catalogue ($M > 5.5$, 1900–2007) (Engdahl & Villaseñor 2002), the catalogue compiled by Wang & Kuo (1995) of all major earthquakes ($M_S > 7.0$) in Taiwan area with recalculated M_S magnitudes (1900–1994), the USGS[1] catalogue ($M > 5$), the homogeneous catalogue (1900–2006) compiled by Chen & Tsai (2008), the TTSN[2] catalogue from IES[3], the CWBSN catalogue from the CWB (Central Weather Bureau) (Shin 1993) and at last the global centroid moment tensor (GCMT[4]) catalogue (1973–2007, $M > 5.0$). We thus cover the period 1900–2007.

Some authors have worked to establish relations between different local magnitudes used in Taiwan over the time (M_H, M_D and M_L), body wave magnitude m_b (1s), surface waves magnitudes M_S and moment magnitude M_W in the Taiwan area (Wang & Chiang 1987; Wang 1992; Chen *et al.* 2007; Chen & Tsai 2008). Indeed, because the definition and procedure for determination of the magnitude differs from one catalogue to another depending on the period considered or on the data used in the calculation, we have decided to normalize all magnitudes with respect to the M_W GCMT (Dziewonski *et al.* 1981) moment magnitude as defined by Kanamori and Hanks (Kanamori 1977; Hanks & Kanamori 1979) through empirical relations (Kanamori & Anderson 1975; Kanamori 1983). This magnitude is adapted to describe the size of earthquakes (Aki 1966; Kanamori 1977).

In this study, we combined all catalogues into one using overlapping. Since the magnitude reported in the different catalogues and the location method and results, especially offshore, vary considerably, we have employed a relatively large magnitude window of ±1.5, a 60-s time window, and an initial location distance of ±150 km. A manual check was done for all earthquakes with magnitudes higher than 6.5 (94 earthquakes). On balance, we have obtained

[1]United States Geological Survey, available on http://neic.usgs.gov/neis/epic/
[2]Available on http://dmc.earth.sinica.edu.tw/
[3]Institute of Earth Sciences, Academia Sinica, Taipei.
[4]Global Centroid moment Tensor available on http://www.globalcmt.org

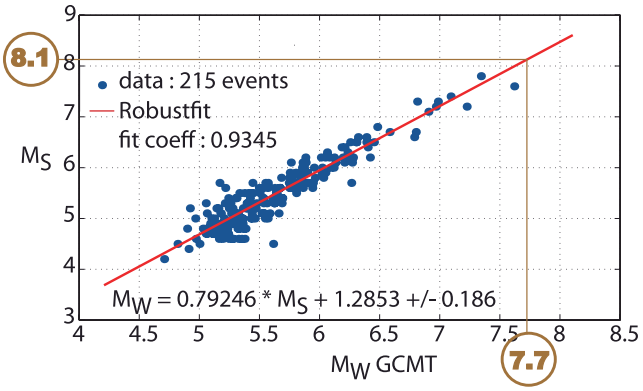

Figure 3. Conversion from M_S magnitude to the GCMT moment magnitude, M'_W. 215 earthquakes between 1973 and 2007 have been used in this regression. 'Robustfit' is a linear regression function from Matlab.

409 374 earthquakes among which 29 had a magnitude higher 7.0 (see Fig. 2 and Table 1); 255 had a magnitude higher than 6.0 and 829 had a magnitude higher than 5.5 (see catalogue online).

We have made the assumption that between magnitude 5.0 and 8.1, the highest magnitude in Taiwan, all magnitudes follow a linear relation and that there's no strong saturation in the different magnitudes used in the conversion (see Fig. S1 in the Supporting Information). We used a linear least-squares regression to establish conversion laws. We defined the M_W GCMT moment magnitude as the independent variable and we considered that the error on this variable is negligible [see Castellaro & Bormann (2007) for discussion]. Finally, we used the Robustfit algorithm from Matlab to do the linear regression. At the end, we used eight relations from surface waves magnitude M_S (Gutenberg 1945; Vanek *et al.* 1962), local magnitude M_L (Shin 1993), local duration magnitude M_D (Tsai *et al.* 1973), body waves magnitude m_b (Gutenberg & Richter 1956), M_{CT} (Chen & Tsai 2008), UK_{GR} (Gutenberg & Richter 1954) and UK_{JMA} (local magnitude from Japan Meteorological Agency) to convert them into M_W GCMT equivalent moment magnitude reference M'_W. Conversion equations used is this study are (see Fig. S1 of the Supporting Information for regression graphs and other equations):

$$M'_W = 0.79246 \times M_S + 1.2853 \pm 0.1860. \quad (1)$$

$$M'_W = 1.0826 \times M_L - 0.5918 \pm 0.2945 \quad (2)$$

(equation 2 is used for M_L and UK_{JMA}, period 1991–2007).

2.2 Revisited magnitude of the 1920 June 5 earthquake

Over the entire instrumental recording period in Taiwan, the 1920 earthquake is the largest in terms of magnitude (see Table S1 in the Supporting Information). Following Wang & Kuo (1995), we used the magnitude from Abe (1981) corrected by addition of 0.06 (Lienkaemper 1984) to be compatible with M_S defined with the Prague Formula (Vanek *et al.* 1962). The surface wave magnitude is estimated at 8.1 (with one-digit precision). We then have used the regression of all available combinations between the surface wave magnitude and the M_W GCMT moment magnitude (i.e. 215 earthquakes) (eq. 1 and Fig. 3). The relation deduced here is similar to that found by Chen *et al.* (2007) even if the choice of the different variables in the regression is different. We finally propose a new equivalent moment magnitude M'_W of 7.7 ± 0.2.

Table 1. List of all earthquakes with equivalent moment magnitude M'_W higher than 7.0 in the window 119.5°E–123°E and 22°–25.5°. Source reference either for the hypocentre location or for the initial magnitude (M_i) used in the conversion: 1: (Engdahl *et al.* 1998; Engdahl & Villaseñor 2002), 2: (Cheng & Yeh 1989), 3: (Cheng *et al.* 1996; Cheng *et al.* 1997), 4: (Wu *et al.* 2008), 5: (Wang & Kuo 1995), 6: (Chen *et al.* 2004), 7: GCMT and 8: (Kao *et al.* 1998). LVF: Longitudinal Valley Faults, SOT: Southern Okinawa Trough.

	Origin time						Hypocentre				Loc. error		Magnitude			
N°	Year	m	day	hr	min	s	Lon.	Lat.	Depth	Ref.	Horiz.	Vert.	M'_W	M_i	Ref	Error
Ryukyu margin																
1	1920	6	5	4	21	35.40	122.080	23.813	35.0	1	10.00	15.00	7.7	M_S 8.1	5	0.19
							122.000	24.000	20.0	2	10.00	15.00				
2	1922	9	1	19	16	9.16	122.040	24.506	35.0	1	10.00	15.00	7.4	M_S 7.7	5	0.19
							122.200	24.600	20.0	2	10.00	15.00				
3	1922	9	14	19	31	42.51	122.644	24.378	35.0	1	10.00	15.00	7.1	M_S 7.3	5	0.19
							122.300	24.600	20.0	2	10.00	15.00				
4	1963	2	13	8	50	4.65	122.060	24.356	35.0	1	10.00	15.00	7.2	M_W 7.2	6	0.00
							122.100	24.400	47.0	2	10.00	15.00				
5	1966	3	12	16	31	19.77	122.695	24.307	28.9	1	10.00	15.00	7.5	M_W 7.5	6	0.00
							122.670	24.240	42.0	2	10.00	15.00				
							122.670	24.240	22.0	8	10.00	15.00				
6	2002	3	31	6	52	49.95	122.163	24.167	16.5	4	0.32	0.38	7.1	M_W 7.1	7	0.00
LVF and Hualien offshore																
7	1951	10	21	21	34	14.00	121.725	23.875	4.0	3	10.00	15.00	7.1	M_S 7.4	5	0.19
8	1951	10	22	3	29	27.00	121.725	24.075	1.0	3	10.00	15.00	7.0	M_S 7.2	5	0.19
9	1951	10	22	5	43	1.00	121.950	23.825	18.0	3	10.00	15.00	7.0	M_S 7.2	5	0.19
10	1951	11	24	18	50	18.00	121.350	23.275	36.0	3	10.00	15.00	7.1	M_S 7.4	5	0.19
11	1957	2	23	20	26	18.02	121.800	23.800	30.0	2	10.00	15.00	7.1	M_S 7.4	5	0.19
12	1972	4	24	9	57	21.43	121.532	23.512	15.4	2	10.00	15.00	7.0	M_W 7.0	6	0.00
13	1986	11	14	21	20	4.52	121.833	23.992	15.0	2	2.60	2.60	7.3	M_W 7.3	7	0.00
							121.760	23.950	33.0	8	10.00	15.00				
SOT																
14	1910	4	12	0	22	13.00	123.000	25.000	200.0	1	10.00	15.00	7.7	M_S 7.4	5	0.19
15	1917	7	4	0	38	20.00	123.000	25.000	0.0	1	10.00	15.00	7.1	M_S 7.4	5	0.19
16	1947	9	26	16	1	57.00	123.000	24.750	110.0	1	10.00	15.00	7.3	M_S 7.6	5	0.19
17	1959	4	26	20	40	38.77	122.792	24.687	126.3	1	10.00	15.00	7.5	M_S 7.9	5	0.19
Huatung Basin earthquakes																
18	1919	12	20	19	33	0.00	122.500	22.500	35.0	1	10.00	15.00	7.0	M_S 7.2	5	0.19
19	1921	4	2	9	36	0.00	123.000	23.000	35.0	1	10.00	15.00	7.1	M_S 7.4	5	0.19
20	1935	9	4	1	37	46.26	121.550	22.500	20.0	2	10.00	15.00	7.1	M_S 7.4	5	0.19
21	1972	1	25	2	6	21.45	122.325	22.549	10.1	1	10.00	15.00	7.3	M_W 7.3	6	0.00
22	1978	12	23	11	23	12.00	122.015	23.224	48.0	1	10.00	15.00	7.0	M_W 7.0	7	0.00
23	1978	7	23	14	42	36.90	121.329	22.352	6.1	2	2.60	2.60	7.2	M_W 7.2	7	0.00
Foreland–Western Taiwan																
24	1935	4	20	22	2	2.86	120.820	24.350	5.0	2	10.00	15.00	7.0	M_S 7.2	5	0.19
25	1941	12	16	19	19	45.66	120.450	23.400	15.0	2	10.00	15.00	7.0	M_S 7.2	5	0.19
26	1999	9	20	17	47	15.85	120.805	23.853	7.0	4	0.30	0.35	7.6	M_W 7.6	7	0.00

3 RELOCATION OF THE M'_W7.7 1920 JUNE 5 EARTHQUAKE FROM ARCHIVE DATA

We propose a simple method to relocate old instrumental earthquakes from picked phase arrival times given in seismological archives using the recent advances in seismological recording by CWBSN (1991–present) and earthquake location methods. Thanks to the CWB of Taiwan archived, which the old seismological bulletin, we determined earthquake location from *S*–*P* arrival time differences.

3.1 Data used

1920 seismograms have disappeared. However, fortunately, archives of the 1920 earthquake were first preserved at TMO and then at the CWB in Taipei in the form of microfilms. A report of a few pages (see Fig. S2 in the Supporting Information) is available for this major earthquake. In 1920, seven stations have recorded the M'_W 7.7 1920 June 5 earthquake (Fig. 2). These stations were located in Taipei (TAP), Taichung (TCU), Tainan (TAI), Taitung (TTN), Hualien (HWA), Hengchun (HEN) and Penghu (PNG). Instruments used at stations TAP, TAI, TTN, PNG, HEN and TCU were Omori seismometers. At HWA, a Portable Tromometer was used (Cheng & Yeh 1989). At that time, station clocks were not synchronous and technicians at the local stations individually adjusted clocks. There were remarkable errors in the arrival times, up to 10 s (Wang 1998), thus resulting in high uncertainties in earthquake location. Studies have shown that time residuals at these stations can be up to 10 s. We consequently used the duration of the 'preliminary tremor' (Table 2), that is, the arrival time difference between *P* and *S* waves (*S*–*P* duration) that we consider as independent of the station clocks.

3.2 Relocation method

The method consists of comparing the set of seven *S–P* durations recorded in 1920 to modern *S–P* times recorded by CWBSN (1991–2008; $M_L \geq 3$; 22°N–25.4°N and 120.9°E–124.5°E). This comparison is possible because nine actual stations are close enough to the seven 1920's stations. CWBSN modern stations are TAP, TAP1, TCU, TAI, TAI1, TTN, HEN, PNG and HWA.

The comparison is done in two steps. First, we identify the high probability area (HPA) where the 1920 earthquake could have occurred by intersecting seven 3-D envelopes, defined for each station. Each envelope is defined by earthquake locations presenting the same *S–P* duration records than those of 1920's ones ($S–P_{1920} \pm$ a tolerance value) (Fig. 4). Secondly, we search all earthquakes with a similar *S–P* duration pattern than those observed in 1920. The tolerance that we give to the residue of the *S–P* duration difference (SP_{RES}) (eq. 3) has been defined as the maximum of the uncertainty on SP_{RES} at each station pair.

$$SP_{RES} = SP_{OBS} - SP_{1920} \quad (3)$$

for a given station pair.

This uncertainty is the sum of the error attributed to (1) picking error and (2) station geographic misfits. Problems inherent to this relocation procedure are the uncertainty estimate on SP_{RES} between 1920 and present. Picking errors depend on phase misidentification, magnification, signal-to-noise ratio and/or the wide band spectral ratio (WSR), instrumentation (short-period or broad-band) and the analyst (training, experience). It is difficult to clearly establish the picking error. According to a model proposed by Zeiler and Velasco (2009), we assume a low picking error on *P* phase of 0.1 s and the double for *S* phase (0.2 s).

Omori seismometers (horizontal pendulum tromometer) were 'highly sensitive to tremors, pulsatory oscillations and comparatively quick period earthquake vibrations' (Omori 1902). Natural period of this instrument was more than 10 s and signals with a period higher than 1 s could be recorded. We do not have seismograms for the 1920 earthquake but picking error associated with this frequency range recording should be large for local events even if we consider big earthquakes. Moreover, from the fact that ground motion is recorded only on horizontal component on Omori seismometers, picking error on *P*-wave first arrival could be higher than 0.5 s. Thus, we add an error associated to the fact that the *P* phase has been picked on a horizontal component. We choose 0.5 s.

In this study, we have estimated SP_{RES} uncertainties by summing picking errors on *P* phase with the errors on *S* phase and with the maximum delay associated to the station geographic misfit (Δt) (eq. 4).

$$\Rightarrow \Delta SP_{RES} = \Delta SP_{OBS} + \Delta SP_{1920} + \Delta t \Rightarrow \Delta SP_{RES} = \Delta P_{OBS} + \Delta S_{OBS} + \Delta P_{1920} + \Delta S_{1920} + \Delta t. \quad (4)$$

Table 3 gives an evaluation of possible uncertainty associated with SP_{RES} for all compared stations. From this table, we can see first that the total uncertainty on SP_{RES} is mainly caused by the picking error except for the TAI1 station. The calculated residue on SP_{RES} for modern earthquakes selected (eq. 3) should not be too far from individual uncertainty (eq. 4). Thus, according to uncertainties on SP_{RES} (Table 3), the best reasonable fit is given ±3 s. Then, we defined the tolerance according to the maximum uncertainty (TAI1, 3.1 s) that we rounded to the closest integer (3 s). So, the HPA is defined by the intersections of all seven *S–P* envelopes defined with SP_{RES} between –3 s and +3 s (Fig. 4).

Within the HPA, we search for an earthquake recorded during instrumental CWB period (1991–2008) that shows the closest *S–P* patterns from the 1920 earthquake. We call these recent earthquakes '1920 analogue-quakes'. To do so, we search for the smallest SP_{RES} at the maximum number of stations (n). All 1920 analogue-quakes are represented, for all C (n,7) with $n \geq 3$ possible stations combinations, as a function of allowed SP_{RES} tolerance (see Fig. S3 in the Supporting Information).

3.3 Results

The extent of the HPA is spatially limited to an area of about 1600 km^2 between 4 and 20 km in depth. This extension is mainly constrained by three stations: HWA (closest station), PNG and HEN (the most distant) (Figs 2 and 4). The HPA is located northeastwards of the earlier determinations for this earthquake, centred around 24.1°N–122.3°E and 12 km in depth (Fig. 4).

Only one 1920 analogue-quake occurred within the HPA and satisfies *S–P* durations at all seven stations with an average SP_{RES} of –0.88 s ($\sigma = 1.55$, max = –2.76) (Table 4). This best modern analogue-quake (1994 October 9 M_L 5.1, with an equivalent moment magnitude M'_W of 4.9 ± 0.3, eq. 2) has been located 50 km eastern offshore Hualien and Suao cities at a depth ranging between 9.1 km (Wu *et al.* 2008) and 12.5 km (Font *et al.* 2004) (Table 4).

To confirm our result, we then check the locations of analogue events satisfying the maximum number of stations allowing for a higher residue (up to ±5 s) – 16 events – and analogues satisfying fewer stations but with better constrained *S–P* residues (up to ±3.0 s) – one event with four stations and residues between –1 s and 1 s. The 16 events are located eastwards and slightly southwards of the HPA between 5 and 39 km depth. The event selected with four stations and with residues between –1 s and 1 s is located within the HPA on the Hoping canyon, west of the Nanao Basin at 6 km depth. The rms of SP_{RES} at all combined stations, for these events, is higher than those of the best analogue selected except for the single former event. However, this event is defined with only four stations. The rms is thus not comparable with an rms calculated with seven stations. Also, SP_{RES} at TCU and PNG stations are important about 4 s and – 4 s. At last, the HWA station, which is restrictive

Table 2. Data from archives used to determine the new location. Questions marks notify that some values were not readable in the archives.

Station name	Longitude	Latitude	First arrival	Duration of preliminary tremor (s) *S–P* duration	Epicentre distance (km)
Taichung–TCU	120°41′	24°09′	12:21:41.?	16.8	125
Hualien–HWA	121°37′	23°58′	12:21:50.0	7.1	52
Taipei–TAP	121°31′	25°02′	12:21:59.6	16.2	120
Tainan–TAI	120°13′	23°00′	12:22:00.0	28.7	213
Hengchun–HEN	120°45′	22°00′	12:22.09.0	33.2	246
Penghu–PNG	119°33′	23°32′	12:22:27.6	35.2	261
Taitung–TTN	121°09′	22°45′	12:2?:31.0	21.8	162

in the location process and the definition of the HPA is not used (Fig. S4 in the Supporting Information). Consequently, this event cannot be selected as a best analogue-quake. Finally, only events selected with 3 s tolerance have a small rms between 1.2 and 2.4 (Figs S3, S4 and Table S2). Among these solutions, our preferred 1920 analogue-quake has the best compromise between number of stations, residue distribution over all stations and rms of SP_{RES}. Two events have an rms smaller than those of the selected analogue but they are defined with fewer station and not constrained by restrictive stations PNG, HEN or HWA (Fig. S4 and Table S2 in the Supporting Information).

4 DISCUSSIONS

4.1 Quality of *S*–*P* duration

Seismograms are lost and it is thus hard to assess the real quality of picking. However, Omori Fusakichi published several papers

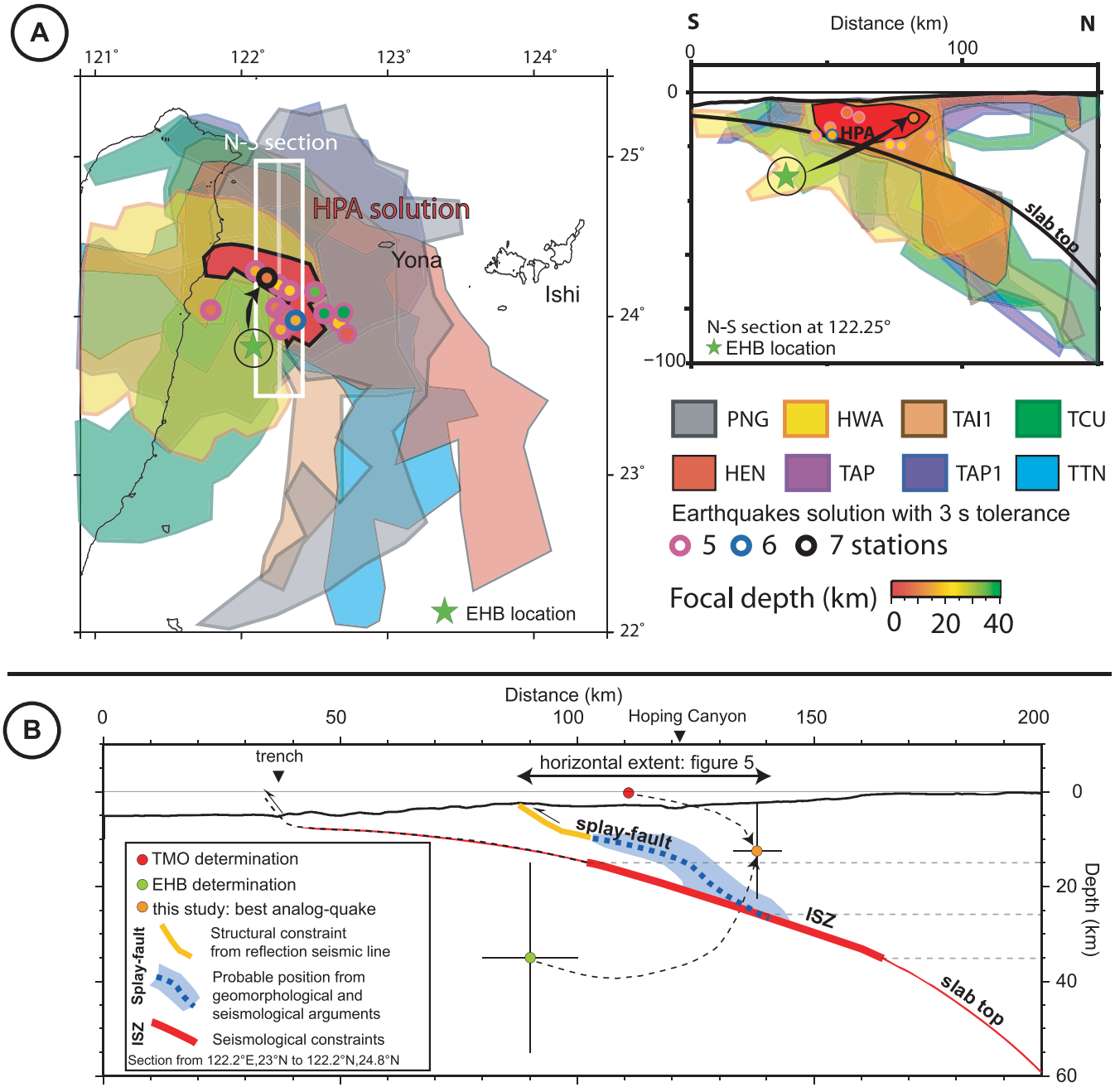

Figure 4. (a) Determination of the high probability area (HPA) where the M'_W 7.7 1920 earthquake occurred and (b) location of the best analogue-quake from Font *et al.* (2004) compared to the position of the ISZ and the possible splay fault. The tolerance for each envelope is ± 3 s (see text for more details). The best '1920 analogue-quake' (1994/10/09) solution is unique. Other earthquakes are selected with the same maximum 3 s tolerance on SP_{RES} but with less correlated stations. The area defined in surface is more extended than in section because all envelopes do not cross in depth to the north. The slab top is built by Font *et al.* (2003) based on wide-angle data. Yona: Yonaguni island, Ishi: Ishigaki island. The splay fault position is constrained by reflection seismic line (Lallemand *et al.* 2010) for its shallow part (yellow line) and by structural and seismological arguments (Font *et al.* 2001; Font & Lallemand 2009) for its deeper part (blue dash line). Seismological constraints for the ISZ come from Kao *et al.* (1998) and Kao (1998). Earthquake location uncertainties are based on seismological studies (Tsai & Wu 1997; Engdahl & Villasenor 2002; Kuochen *et al.* 2004; Font & Lallemand 2009).

Table 3. Evaluation of uncertainties on SP_{RES}. For each station, uncertainty is given by eq. (2), that is, by summing the errors associated with the geographic misfit (stations error) and picking errors on *P* and *S* waves. Information about stations comes from the bulletin written by Cheng and Yeh (1989). All station coordinates are given in the WGS-84 referential. Precision is about 100 m for station position. To calculate the maximum delay due to the geographic station misfit, a low *P*-wave velocity of 3 km s^{-1} and a high V_P/V_S ratio of 2 have been used.

STATION 1920	CWBSN stations	Station error		Picking error (s)		Uncertainty (s)
		Geo. misfit (m)	Max. delay (s)	1920	Recent	
1: TAP	TAP1	100	0.03	0.5 + 0.2 + 0.1	0.2 + 0.1	1.13
	TAP	10	0.003			1.10
2: TCU	TCU	250	0.08			1.18
3: TAI	TAI	165	0.06			1.16
	TAI1	6100	2.0			3.1
4: TTN	TTN	30	0.01			1.11
5: HWA	HWA	135	0.05			1.15
6: HEN	HEN	130	0.05			1.15
7: PNG	PNG	60	0.02			1.12

Table 4. Best modern analogue-quake presenting the same characteristics in term of *S–P* arrival time difference at selected stations as 1920 earthquake. This best 1920 analogue-quake is the M'_W 4.9 on 1994 October 9. The TAP1 station is not used in statistic calculation because it is located in a well and the surface TAP station is available. Mean and residual mean square (rms) of SPRES is −0.884 s and 1.556 s, respectively. The two early proposed locations for the 1920 earthquake are reminded. Hypocentre determinations of the best analogue are given by the CWB, Wu *et al.* (2008) and Font *et al.* (2004).

Comparison of 1920 *S–P* pattern with the best modern analogue earthquake selected				
Station		$SP_{observed}$ (s)	$SP_{RES} = SP_{observed} - SP_{1920}$ (s)	First arrival
1- HWA		7.94	0.84	07:42:09.45
2- TAP	TAP1	15.91	–0.29 (not used)	07:42:15.57
	TAP	13.40	–2.80	07:42:15.98
3- TCU		18.47	1.67	07:42:21.51
4- TTN		21.04	–0.76	07:42:28.64
5- TAI	TAI1	25.94	–2.76	07:42:33.31
	TAI	–	–	07:42:33.14
6- PNG		33.83	–1.37	07:42:35.73
7- HEN		32.19	–1.01	07:42:38.46
Location of the M'_W 7.7 1920 earthquake				
Location source		Latitude (°N)	Longitude (°E)	Depth (km)
1920	TMO	24.0000	122.0000	–
	EHB	23.8130	122.0800	35
Analogue	CWB	24.2417	122.1841	10
	[Wu *et al.* 2008]	24.2363	122.2175	9.1
	MAXI [Font *et al.* 2004]	24.2458	122.1988	12.5

at the beginning of the 20th century where he showed that it was possible to measure preliminary tremor for near earthquakes (with $T < 0.7$ s and within 300 km) using Omori seismometer (Wood 1914; Davison 1924). The relation between the duration of preliminary tremor and the epicentral distance in near field has been shown (Omori 1907, 1920; Imamura 1922). Later, preliminary tremor has been considered like being *S–P* delay time. Omori horizontal pendulums used on Taiwan Island in 1920 had two components (N–S and E–W), their natural period was 10–15 s, the magnification was 20 and the damping was 2–3 (Hsiao N.-C., CWB, personal communication, 2010). The driving rate of recording paper is unknown from our knowledge. For comparison, with similar instruments, preliminary tremors at few near stations have been identified in 1923 in Japan with a similar earthquake to the 1920 earthquake. Indeed, the M_W 7.9 1923 Kanto earthquake occurred on the plate interface at shallow depth along the northernmost part of the Sagami Trough in the Sagami Bay where the PSP is being subducted beneath Honshu Island. With a moment magnitude similar to the 1920 earthquake (Pacheco & Sykes 1992) and similar distance to seismic stations (within 300 km), preliminary tremor have been picked and the epicentral distance has been determined from these data (Jaggar 1923; Imamura 1924). According to the rupture velocity, classically between 2 and 3.5 km s^{-1}, an overlapping between *P* waves, originated from other asperities along the plate interface during the rupture or from waves propagation dispersion, and *S* waves certainly occurred. However, seismometer characteristics, in particular recording on horizontal components, instrumental response below relatively high natural period of 20 s (*S* waves are classically characterized by longer periods than *P* waves) and the relatively small magnification, can explain that it was possible to separate *S* from *P* phases.

4.2 Location method and result

This work is based on the assumption that the fault that triggered the 1920 earthquake has generated, during the instrumental catalogue, at least one analogue-quake. If this analogue-quake is close enough to the 1920 earthquake, then the *S–P* pattern on the

modern equivalent stations should be similar. It also implies that this analogue earthquake should be large enough to be recorded by all seven station. Moreover, the shape of each tolerance envelope depends on the distribution of hypocentres and we cannot be sure that the final domain which defines the HPA is more extended (a seismic gap currently exists) or not. Our analysis provides results that either constrain *S–P* durations at the seven stations (with a relatively high tolerance on SP_{RES} of 3 s) or constrain *S–P* durations at fewer stations but with a smaller tolerance of 1 s. Because PNG, HEN and HWA are restrictive to define the HPA, the first set of constraints allowed us to select one event from the instrumental catalogue (∼17 yr of observation). Based on the available data, it is difficult to definitely solve the exact 1920 earthquake location. However, all possible hypocentre determinations are clearly NNE and shallower than the previous locations.

4.3 Candidate faults

Along the Ryukyu margin, east of Hualien, several faults have been reported to cut through both the upper and the subducting plate. To determine which fault has the highest probability of being involved in the occurrence of the 1920 earthquake, we have used three criteria: (1) we compare the maximum possible magnitude along candidate faults with the estimated dislocation associated with the 1920 earthquake, (2) we compare the depth of the HPA with that of the best 1920 analogue-quake according to the geometry of these faults, and lastly, (3) we use information of the seismological bulletin about a minor tsunami to discuss about the source. A broad view of the criteria's fits for each candidate fault is given in Table 5. Note that no aftershock information, which could have helped us to constrain the fault plane, has been recovered from the archives.

4.4 Fault geometry

From the revised magnitude, it is possible to make reasonable assumptions about the surface rupture using the elastic dislocation theory (Kanamori & Anderson 1975; Aki & Richards 1980). The moment magnitude of an earthquake is given by the equation of Hanks and Kanamori (Hanks & Kanamori 1979): $M_W = \frac{2}{3}[\log(M_0) - 9.1]$. The moment M_0 is defined as $M_0 = \mu DS$ where μ is the rigidity ($N\,m^{-2}$), D the mean slip (m) and S the surface rupture (m^2). The average slip depends on the type and length of this fault (Wells & Coppersmith 1994; Wang & Ou 1998; Fujii & Matsu'ura 2000). Considering a length lower than 200 km, the average slip reaches a maximum of 3 m for an intraplate strike-slip event and 5 m for an island-arc inter-plate thrust event (Fujii & Matsu'ura 2000). Assuming a rigidity of 3.5×10^{10} $N\,m^{-2}$ for a continental crust as suspected for the Ryukyu arc the surface rupture for a magnitude 7.7 ± 0.2 should range between 2100 km^2 (7.5 with 3 m average slip) and 5100 km^2 (7.9 with 5 m average slip).

Let us first consider the ISZ as a candidate fault. Based on the distribution of the seismicity (Kao & Rau 1999; Wu *et al.* 2009), we have considered the Hsincheng Ridge as the western limit of the ISZ and the northern extent of the Gagua Ridge as the eastern limit assuming that the ridge acts as a seismic barrier (Fig. 5). We have considered also the ISZ updip limit to 15 km (shallow intersection between the upper crust and the downgoing PSP) (Wang *et al.* 2001) and the ISZ downdip limit to 35 km depth (Kao 1998). Considering a mean dip angle of the subducting PSP of about 20° (Font *et al.* 2003), the ISZ extent is 120 km long over 60 km width. Given this geometry (Fig. 5), the highest possible moment magnitude is 8.0 (with 5 m average slip). With such limits, if the ISZ has entirely slipped during the 1920 earthquake then the average slip would range between 0.9 m (*M* 7.5) and 3.5 m (*M* 7.9).

Regarding the splay-fault hypothesis affecting the Ryukyu upper plate, the E–W horizontal extent of the Hoping seismicity cluster (Font & Lallemand 2009) is supposed to outline the length of the fault whereas the downdip width should be less than those of the ISZ because it is steeper. Considering this geometry, the extent is 60 km in length and about 55 km in width with a mean dip angle of 26° (Figs 4 and 5). With a rupture along the whole surface of the splay fault, the highest possible magnitude reaches 7.6 with

Table 5. Comparison of criteria on candidate faults. The fault geometry is compared in terms of (1) possible rupture area, maximal moment magnitude and maximal possible average slip specific to the size and nature of the considered fault; (2) depth according to the depth range of the HPA and depth of the best 1920 analogue-quake; (3) tsunami triggering. S: maximum rupture surface (km^2); U: updip limit (km); D: Downdip limit (km); M_{max}: maximal moment magnitude with 3 m (max. average slip for splay-fault and strike-slip fault) and 5 m (max. average slip for ISZ and ELA fault) of average slip; slip* (m): required average slip for a whole rupture with *M* 7.7 ± 0.2 (a value for *M* 7.5 and the other for *M* 7.9). - / - - / - - - low, very low, extremely low probability; + / + + / + + + compatible, very compatible, in perfect agreement.

Discrimination criterions		Candidate Faults							
		ISZ		Splay-fault		N-S Strike-slip fault		ELA fault	
		S: 7200 (120x60) M_{max}: 8.0 U: 15, D: 35		S: 3000 (60x50) M_{max}: 7.63 U: 0, D: 30		S: 3000 (100x30) M_{max}: 7.6 U: 0, D: 30		S: 4400 (110x40) M_{max}: 7.86 U: 20, D: 40	
		Slip*: 0.9	Slip*: 3.5	Slip*: 1.9	Slip*: 7.7	Slip*: 2.1	Slip*: 8.5	Slip*: 1.5	Slip*: 5.8
1	S: 1300 - 5100	+ + +		+ + +		+ + +		+ + +	
	$M'_W = 7.7 \pm 0.2$	+ + +		+		+		++	
	Max. average slip	+ + +	+ + +	+ + +	- - -	+ + +	- - -	+ + +	+
2	Depth range of the HPA 4-20 km	+ + +		+ + +		+ + +		- - -	
	Depth of the best analog-quake:12.5 km	-		+ + +		+ + +		- - -	
3	Tsunami triggering	+ +		+ + +		+ +		-	

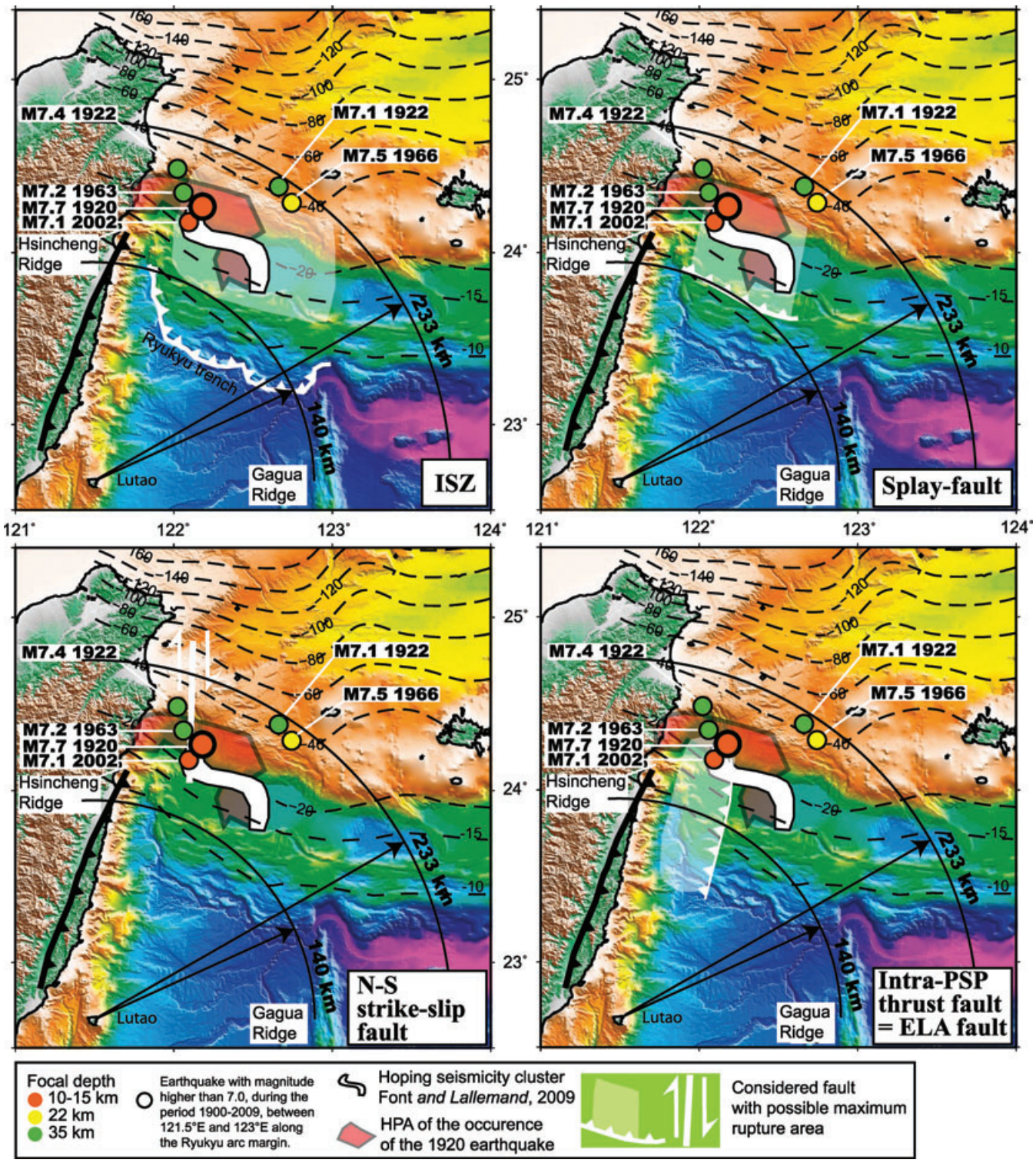

Figure 5. The M'_W 7.7 1920 earthquake is represented with its revised hypocentre and candidate active faults. Other major earthquakes (1900–2009) that occurred on the Ryukyu margin are also represented. Assumption is made on the best available location for each earthquake. The location of the M'_W 7.1 2002 is given by 3-D determination using MAXI process (Font *et al.* 2004), the location of the M'_W 7.2 1963, the M'_W 7.1 1922 and the M'_W 7.4 1922 earthquakes come from the EHB process. At last, the location of the M'_W 7.5 1966 earthquake is given by Kao *et al.* (1998). The arc of about 200 km circle centred on Lutao Island (see text) is reported in the Ryukyu arc area. It represents the source area of the tsunami.

an adapted 3 m average slip according to the fault length (Fujii & Matsu'ura 2000). With such limits, if the splay fault has entirely slipped during the 1920 earthquake then the average slip would range between 1.9 m (*M* 7.5) and 7.7 m (*M* 7.9).

The N–S strike-slip fault zone close to Taiwan, that should accommodate the southern Okinawa trough rifting (Lallemand & Liu 1998), is supposed to have a downdip limit not deeper than the arc Moho depth (i.e. 30 km) and a length of about 100 km.

Then, the expected maximum moment magnitude should be 7.6 (with 3 m average slip). With such limits, if the N–S strike-slip fault has entirely slipped during the 1920 earthquake then the average slip would range between 2.1 m (M 7.5) and 8.5 m (M 7.9).

Considering the deformation of the PSP, the suspected intraslab N–S reverse fault located east of the Luzon arc continuity (ELA fault) could have a width of 40 km and a ∼N–S extension of 110 km as given by Font (2002). The expected maximum moment magnitude should thus be 7.86 (with 5 m average slip). With such limits, if the ELA fault has entirely slipped during the 1920 earthquake then the average slip would range between 1.5 m (M 7.5) and 5.8 m (M 7.9).

As a consequence of these geometries and parameters of the rupture, each candidate fault has an extent enough to generate an earthquake with a magnitude equivalent to the range of those of the 1920 earthquake. However, a huge, and certainly improbable, average slip is needed on the splay fault and the N–S strike-slip fault to be in agreement with the highest possible magnitude of the 1920 earthquake according to our uncertainty.

4.5 Probable 1920 earthquake depth versus candidate faults depth

The depth range of the HPA is between 4 and 20 km. As a consequence, it does not support the hypothesis of a rupture within the subducting PSP. We thus discard the ELA fault. Regarding faults that involve the upper plate, we can use the location of the best 1920 analogue-quake that we have selected to discriminate among other faults. However, depth is a difficult parameter to constrain especially offshore (Font *et al.* 2004) and the location of this single solution has to be used cautiously because we have assumed that it is the unique best 1920 analogue-quake (see previous discussion). So, the HPA stays a better criterion than the depth of the best analogue-quake.

The location of the best analogue-quake seems relatively well constrained and we assume that we can use its depth to support our arguments. The best selected 1920 analogue-quake, that is, the M'_{W} 4.9 1994 earthquake, occurred offshore about 60 km east of Hualien on the west part of the Hoping seismicity cluster (Font & Lallemand 2009). Unfortunately, the focal mechanism of this earthquake is not mentioned among BATS solutions, GCMT solutions or in the recent studies, (i.e. Wu *et al.* 2008). This analogue-quake is located at a distance of 100 ± 5 km from the trench and at 12.5 ± 10 km depth. At the epicentral position of the analogue-quake, the ISZ depth is given at 26 km according to the geometry proposed by Font *et al.* 2003 (Fig. 4B). Taking into consideration the large location uncertainties of the offshore earthquake and the structural configuration, the ISZ does not seem to be the best candidate for the rupture of the 1920 earthquake. On the contrary, the splay fault and the N–S strike-slip fault zone appear more compatible with the hypocentre determination even if the splay fault is considered the nucleation would be on its downdip limit (Figs 4 and 5).

4.6 Triggered tsunami?

The earthquake bulletin relates the story of a fisherman that was sailing near Lutao Island when earthquake occurred (Fig. 5). The translation of the ship's report can be found in the Supporting Information. The story reveals that a relatively high-frequency vibration has shaken the boat for 2 min at 12 h 31 (relative to seismic station clock), which means about 10 min after first arrivals recorded in Taiwan. It is not possible that these high-frequency waves came from the 1920 mainshock and it is difficult to really know what is the source even if it could certainly be caused by an aftershock. Soon after 12 h 33, more than 12 min after the 1920 mainshock, long period water waves came from the NE. Their importance according to the feeling of the fisherman supports the hypothesis that a significant seafloor vertical motion, or at least the displacement of a huge volume of rocks or sediments, occurred. According to a mean depth about 4000 m between Lutao and the Ryukyu arc, the velocity of such water waves should be about 700 km h^{-1} using the basic equation $v = \sqrt{g \cdot h}$ where v is the velocity, g the acceleration due to gravity and h the water depth (Zhang *et al.* 2009). With such velocity, the source must be located at a distance between 140 km (with a minimum 12 min delay) and 233 km (with an assumed maximum 20 min delay) from the position of the fisherman (see also Fig. S5 in the Supporting Information for more details). If the fisherman was close to Lutao (despite wrong coordinates), then the source of the long-period water waves coincides with the Ryukyu forearc (Fig. 5). The problem comes from the fact that no other report is given in the TMO archives and no references have been found about an historical tsunami caused by the 1920 earthquake (Ma & Lee 1997), but it is also true that no tide-gauge station was installed in 1920. So we have to consider that a minor tsunami, which originated from the Ryukyu forearc (Fig. 5), hit the east coast of Taiwan as suggested by the fisherman.

Historical tsunamis, the sources of which were located on the Ryukyu margin, were reported on the east coast of Taiwan. The best selected 1920 analogue-quake did not trigger any tsunami but its magnitude was relatively small (M'_{W}4.9). This analogue-quake was very close (∼10 km and equivalent depth) to the M'_{W} 7.1 2002 March 31 earthquake which was a reverse fault associated with the Ryukyu subduction that occurred at 122.076°E–24.2°N at 15 km depth after relocation using MAXI method (Font *et al.* 2004). For comparison, this M'_{W} 7.1 2002 earthquake has triggered a tsunami of 20 cm (peak-to-trough) that was recorded on Yonaguni Island and at Suao City but not on Ishigaki Island, which is further east (Chen *et al.* 2005). It is surprising that a M'_{W} 7.7 earthquake that releases eight times the energy of a M'_{W} 7.1 earthquake did not trigger any tsunami except those minor ones reported only by the fisherman. However, local tsunami runup does not depend only on M_0 value. It also depends on the geometry of the fault, the slip distribution along the fault area (presence or lack of subsurface rupture, depth of the maximum slip) and the overlying water depth (Geist *et al.* 2006).

Another event, the M'_{W} 7.5 1966 earthquake (24.24°N–122.67°E, 22 km depth) (Kao *et al.* 1998), triggered a tsunami of about 50 cm near Ilan City on the east coast of Taiwan and killed seven people (Ma & Lee 1997). This tsunami has been generated by a strike-slip earthquake according to its focal mechanism (Wu 1970; Wu 1978; Pezzopane & Wesnousky 1989; Kao *et al.* 1998). The water depth above the hypocentre was about 700 m and thus favoured tsunami generation.

4.7 Selection of the best candidate fault

On one side, we have information about the most probable location and the moment magnitude which do not allow us to completely discriminate between candidate faults. Indeed, the shallow depth (4–20 km) of the HPA is in favour of a shallow earthquake involving either the ISZ or a fault cutting through the upper plate (splay fault or N–S strike-slip fault), whereas the depth of the best analogue-quake rather supports the fault within the upper plate, even if the

required average slip along these faults is certainly too large. The geometry of the ISZ seems to be more adapted but the depth of the best analogue-quake is not in agreement (Table 5).

On the other side, the minor reported tsunami on Lutao Island though the lack of reported tsunami on the east coast of Taiwan or in Yaeyama Islands suggests a small seafloor displacement below an important water depth above the maximum slip area. In this case, the splay fault seems to be the best candidate fault (Table 5). Because the required average slip on the splay fault alone seems too large, the best compromise would be to consider a rupture on the splay fault with a minor seafloor displacement, explaining the shallow nucleation as given by the location of the best analogue-quake, followed by a downward and lateral propagation of the rupture along the ISZ.

4.8 Interplate coupling

Over the last century, six major earthquakes occurred in the Ryukyu forearc between Taiwan and the Gagua Ridge (Fig. 2, Table 1). Among them, as mentioned above, the M'_W 7.5 1966 earthquake probably occurred within the upper plate along a strike-slip fault. Two others, close to each other, have a reverse fault mechanism: the M'_W 7.2 1963 earthquake (Katsumata & Sykes 1969; Chen *et al.* 2004) and the M'_W 7.1 2002 earthquake that could have nucleated on the ISZ or on the splay fault. Among the other three, the doubt is possible and there are no final arguments at this moment to definitively decide which fault is involved. First, the 1920 earthquake could possibly be attributed to the splay fault and the ISZ (see discussion above). The two last earthquakes have to be elucidated, that is, the M'_W 7.4 1922 Ilan earthquake (20–35 km depth) (Nakamura 1922) and the M'_W7.1 1922 (20–35 km depth). It is necessary to relocate and to study these two events before concluding about the faults that can be involved. We thus cannot exclude that the two 1922 earthquakes also occurred on the ISZ or the splay fault. However, it should be very improbable that three major earthquakes (1920, 1922 and 1922) occurred successively in two years on the same small portion of a fault. Nevertheless, at the extreme case, five events may be associated with the ISZ or the splay fault.

We can now estimate the seismic coupling, that is, the ratio of average seismic slip rate to plate convergence (Scholz 1990, 1998), to discuss the seismic hazard along the segment of the ISZ close to Taiwan. In our case, we consider events either located on the ISZ or on the splay fault. This ratio depends especially on the recurrence of major earthquakes. Over 108 years, considering that three events (1920, 1966 and 2002) occurred on the ISZ and considering a convergence rate of about 10.7 cm yr^{-1} (Lallemand & Liu 1998), the seismic coupling coefficient is about 0.2 according to our geometry. This value increases to 0.27 if we also consider the two 1922 earthquakes (see discussion above). This value increases to a maximum of 0.4 considering seismicity with magnitude lower than seven. It is a relatively low value, which indicates either a stable state of aseismic slip with few interface earthquakes or elastic strain accumulation before a M 8.1 earthquake. In such case, the resultant accumulated slip would amount to 7 m according to our geometry. No such big earthquake has been reported historically and recent studies have showed that aseismic slip (Nakamura 2009) occurred in this region between 122.5°E and 123.3°E and between 30 and 60 km depth. We thus assume that the Ryukyu subduction close to Taiwan shows a relatively weak interplate coupling. It is rather characterized by recurrent earthquakes, with magnitudes higher than 7 but lower than 8, especially located in the Hoping Seismicity cluster between 122°E and 122.5°E at shallow depths (0–30 km).

5 CONCLUSION AND PROSPECTS

We propose in this study a relative location technique to improve hypocentre determination of largest early instrumental earthquakes. This method can be applied to earthquakes for which *P*- and *S*-wave arrival times are available in seismological bulletins or directly from reading old seismograms and for which the present seismic network is installed close to the early network. We applied this method to relocate the biggest known earthquake in Taiwan. The earthquake location proposed in this study is in better agreement with main faults known offshore eastern Taiwan compared with previous published determination.

Using a catalogue over the period 1900–2007 for the Taiwan area, we have calculated a new equivalent moment magnitude for all earthquakes during the instrumental period. A revised moment magnitude of 7.7 ± 0.2 for the 1920 June 5 earthquake is proposed.

The M'_W 7.7 1920 earthquake probably occurred on the west part of the Hoping seismicity cluster. The rupture probably occurred along the ISZ with a shallow nucleation possibly along a splay fault followed by a downward and lateral propagation of the rupture that would explain the lack of significant seafloor motion and subsequent tsunami. According to the seismic coupling coefficient which can be calculated over 108 years of seismicity, we assume that the Ryukyu subduction close to Taiwan shows a relatively weak interplate coupling and it is rather characterized by recurrent earthquakes, with magnitudes higher than 7 but lower than 8, especially located in the Hoping Seismicity cluster between 122°E and 122.5°E at shallow depths (5–30 km).

This approach should be extended to other historical earthquakes with magnitude higher than six to fully describe the seismotectonic context and seismic hazard of this area. Also, a better knowledge of the fault geometries, in particular the ISZ, is still necessary.

ACKNOWLEDGMENTS

The authors wish to thank the Central Weather Bureau (CWB, Taiwan) and the IES (Institute of Earth Sciences) at the Academia Sinica (Taipei, Taiwan) represented by Bor-Minh Jahn for providing the archives about the 1920 earthquake. We want also to thank translators of the archives at IES: Mu Chung-Shiang and Dr Ya-Chuan Lai for her help in the bibliographical search. Also, we thank Antonio Villasenor and Bob Engdahl to spend time in testing revised location and Hélène Hebert to spend time to evaluate tsunami traveltimes. This paper was much improved by comments from the two anonymous reviewers. This work was supported by the NSC (National Science Council via ORCHID program) and the 'F-Taiwan foundation' managed by the French 'Academie des sciences' for the travel support, and the ANR (Agence Nationale pour la Recherche) through the ACTS-Taiwan (Active Tectonics and Seismic Hazard in Taiwan) project for the working budget. We also acknowledge the LIA (Associated International Laboratory) ADEPT (Active Deformation and Environment Program for Taiwan) and its co-directors, late Jacques Angelier, and Bor-Minh Jahn for other financial help. For their constant help, we acknowledge the FIT (French Institute in Taipei) and the BRT (Bureau de Representation de Taipei). Some figures and the tsunami traveltimes map have been made using respectively the open GMT software of Paul Wessel and Walter H.F. Smith and the Geoware Tsunami TTT software of Paul Wessel.

REFERENCES

Abe, K., 1981. Magnitudes of large shallow earthquakes from 1904 to 1980, *Phys. Earth planet. Inter.,* **27,** 72–92.

Aki, K., 1966. Generation and propagation of g-waves from the Niigata earthquake of June 16, 1964-pt. 2, estimation of earthquake moment, released energy, and stress-strain drop from the g wave spectrum, *Bull. Earthq. Res. Inst. Tokyo Daigaku Jishin Kenkyusho Iho,* **44,** Part 1, 73–88.

Aki, K. & Richards, P.G., 1980. *Quantitative Seismology: Theory and Methods*, University Science Books, Sausalito, CA.

Amante, C. & Eakins, B.W., 2009. ETOPO1 1 Arc-minute global relief model: procedures, data sources and analysis, NOAA Technical Memorandum NESDIS NGDC-24, 19 pp, March 2009.

Biq, C., 1972. Dual-trench structure in the Taiwan-Luzon region, *Proc. Geol. Soc. China,* **15,** 65–75.

Bird, P., 2003. An updated digital model of plate boundaries, *Geochem. Geophys. Geosyst.,* **4**(3), 1027, doi:10.1029/2001GC000252.

Bos, A.G., Spakman, W. & Nyst, M.C.J., 2003. Surface deformation and tectonic setting of Taiwan inferred from a GPS velocity field, *J. geophys. Res.,* **108**(B10), 2458, doi:10.1029/2002JB002336.

Castellaro, S. & Bormann, P., 2007. Performance of different regression procedures on the magnitude conversion problem, *Bull. seism. Soc. Am.,* **97**(4), 1167–1175.

Chai, B.H.T., 1972. Structure and tectonic evolution of Taiwan, *Am. J. Sc.,* **272**(5), 389–422.

Chemenda, A.I., Yang, R.K., Hsieh, C.H. & Groholsky, A.L., 1997. Evolutionary model for the Taiwan collision based on physical modelling, *Tectonophysics,* **274**(1–3), 253–274.

Chemenda, A.I., Yang, R.K., Stephan, J.F., Konstantinovskaya, E.A. & Ivanov, G. M., 2001. New results from physical modelling of arc-continent collision in Taiwan: evolutionary model, *Tectonophysics,* **333**(1–2), 159–178.

Chen, K.-P. & Tsai, Y.B., 2008. A catalog of Taiwan earthquakes (1900–2006) with homogenized Mw magnitudes, *Bull. seism. Soc. Am.,* **98**(1), 483–489, doi:10.1785/0120070136.

Chen, P.-F., Ekstrom, G. & Okal, E.A., 2004. Centroid moment tensor solutions for Taiwan earthquakes of the WWSSN era (1963–1975), *Diqiu Kexue Jikan = TAO, Terrestrial,Atmospheric and Oceanic Sciences,* **51**(1) 61–73.

Chen, J.-H., Chen, P.-F., Hsiao, N.-C. & Chang, C.H., 2005. Tsunami arrival time database and warning system in Taiwan, International Workshop on Emergency Response and Rescue. Taipei, 2005.

Chen, K.-C., Huang, W.-G. & Wang, J.-H., 2007. Relationships among magnitudes and seismic moment od earthquakes in the Taiwan region, *Terr. atmos. Oceanic Sci.,* **18**(5), 951–973.

Chen, K.H., Toda, S. & Rau, R.-J., 2008. A leaping, triggered sequence along a segmented fault: the 1951 M (sub L) 7.3 Hualien-Taitung earthquake sequence in eastern Taiwan, *J. geophys. Res.,* **113,** B02304, doi:10.1029/2007JB005048.

Chen, R.-Y., Kao, H., Liang, W.-T., Shin, T.-C., Tsai, Y.-B. & Huang, B.-S. *, 2009.* Three-dimensional patterns of seismic deformation in the Taiwan region with special implication from the 1999 Chi-chi earthquake sequence*, Tectonophysics,* **466**(3–4), 140–151.

Cheng, S.-N. & Yeh, Y.-T., 1989. *Catalog of the Earthquakes in Taiwan from 1604 to 1988.* Bulletin IES, R-661, 255pp., Institute of Earth Sciences, Taipei.

Cheng, S.-N., Yeh, Y.-T. & Yu, M.-S., 1996. The 1951 Taitung earthquake in Taiwan, *J. geol. Soc. China,* **39**(3), 267–285.

Cheng, S.-N., Yu, T.-T., Yeh, Y. T. & Chang, Z.-S., 1997. Relocation of the 1951 Hualien, Taitung earthquake sequence, in *Proceedings of Meteorology, Conference on Weather Analysis and Forecasting,* pp. 690–699, Central Weather Bureau, Taipei.

Chou, H.-C., Kuo, B.-Y., Hung, S.-H., Chiao, L.-Y., Zhao, D. & Wu, Y.-M., 2006. The Taiwan-Ryuku subduction-collision complex: folding of viscoelastic slab and the double seismic zone, *J. geophys. Res.,* **111**(B4410), doi:10.1029/2005JB03822.

Chung, L.-H., Chen, Y.-G., Wu, Y.-M., Shyu, J. B. H., Kuo, Y.-T. & Lin, Y.-N.N., 2008. Seismogenic faults along the major suture of the plate boundary deduced by dislocation modeling of coseismic displacements of the 1951 M7.3 Hualien-Taitung earthquake sequence in eastern Taiwan, *Earth planet. Sci. Lett.,* **269**(3–4), 415–425.

Davison, C., 1924. Fusakichi Omori and his work on earthquakes, *Bull. seism. Soc. Am.,* **14**(4), 240–255.

Dziewonski, A.M., Chou, T.A. & Woodhouse, J.H., 1981. Determination of earthquake source parameters from waveform data for studies of global and regional seismicity, *J. geophys. Res.,* **86**(B4), 2825–2852.

Engdahl, E.R. & Villaseñor, A., 2002. Global seismicity : 1900–1999, *Inter. Handbook Earthq. Eng. Seism.,* **81A,** 665–689.

Engdahl, E.R., Van Der Hilst, R.D. & Buland, R.P., 1998. Global teleseismic earthquake relocation with improved travel times and procedures for depth determination, *Bull. seism. Soc. Am.,* **88**(3), 722–743.

Font, Y., 2002. Contribution to the understanding of the westernmost Ryukyu subduction termination into the active arc-continent collision of Taiwan; new insights from seismic reflection analyses and earthquake relocation, *PhD thesis,* Universite des Sciences et Techniques du Languedoc, Montpellier, France.

Font, Y. & Lallemand, S., 2009. Subducting oceanic high causes compressional faulting in southernmost Ryukyu forearc a revealed by hypocentral determinations of earthquakes and reflection/refraction seismic data*, Tectonophysics,* **466**(3–4), 255–267.

Font, Y., Lallemand, S. & Angelier, J., 1999. Etude de la transition entre l'orogene actif de Taiwan et la subduction des Ryukyu; apport de la sismicite. Transition between the active orogen of Taiwan and the Ryukyu subduction; a new insight from seismicity, *Bulletin de la Societe Geologique de France,* **170**(3), 271–283.

Font, Y., Liu, C.-S., Schnurle, P. & Lallemand, S., 2001. Constraints on backstop geometry of the Southwest Ryukyu subduction based on reflection seismic data, *Tectonophysics,* **333**(1–2), 135–158.

Font, Y., Kao, H., Liu, C.-S. & Chiao, L.-Y., 2003. A comprehensive 3D seismic velocity model for the eastern Taiwan-southernmost Ryukyu regions, *Diqiu Kexue Jikan = TAO, Terrestrial, Atmospheric and Oceanic Sciences,* **41**(2), 159–182.

Font, Y., Kao, H., Lallemand, S., Liu, C.-S. & Chiao, L.-Y., 2004. Hypocentre determination offshore of eastern Taiwan using the maximum intersection method, *Geophys. J. Int.,* **158**(2), 655–675.

Fujii, Y. & Matsu'ura, M., 2000. Regional difference in scaling laws for large earthquakes and its tectonic implication, *Pure appl. Geophys.,* **157**(11–12), 2283–2302.

Geist, E.L., Bilek, S.L., Arcas, D. & Titov, V.V., 2006. Differences in tsunami generation between the December 26, 2004 and March 28, 2005 Sumatra earthquakes, *Earth planet. Sci. Lett.,* **58,** 185–193.

Gutenberg, B., 1945. Amplitudes of surface waves and magnitudes of shallow earthquakes, *Bull. seism. Soc. Am.,* **35**(1), 3–12.

Gutenberg, B. & Richter, C.F., 1954. *Seismicity of the Earth and Associated Phenomena,* Princeton University Press, Princeton.

Gutenberg, B. & Richter, C.F., 1956. Magnitude and energy of eathquakes, *Ann. Geofis.,* **9,** 1–15.

Hanks, T.C. & Kanamori, H., 1979. A moment magnitude scale, *J. geophys. Res.,* **84**(B5), 2348–2350.

Hsu, M.T., 1961. Seismicity of Taiwan (Formosa), *Bull. earthq. Res. Inst. Tokyo University,* **39,** 831–847.

Hsu, M.T., 1980. *Earthquake Catalog in Taiwan (from 1644 to 1979). Bulletin NTU. E. E. Center. Taipei,* 77pp., National Taiwan University, Taipei.

Hsu, S.-K., 2001. Lithospheric structure, buoyancy and coupling across the southernmost Ryukyu subduction zone: an example of decreasing plate coupling, *Earth planet. Sci. Lett.,* **186**(3–4), 471–478.

Imamura, A., 1922. On the relation of the duration of the preliminary tremor to the epicentral distance, *Imp. Earthq. Investigation Com, B,* **9**(96), 108–117.

Imamura, A., 1924. Preliminary note on the great earthquake of southeastern Japan on September 1, 1923, *Bull. Seismol. Soc. Am.,* **14**(2), 136–149.

Jaggar, T.A., 1923. The Yokohama-Tokyo earthquake of September 1, 1923, *Bull. Seismol. Soc. Am.,* **13**(4), 124–146.

Kanamori, H., 1977. The energy release in great earthquakes, *J. geophys. Res.,* **82**(20), 2981–2987.

Kanamori, H., 1983. Magnitude scale and quantification of earthquakes, *Tectonophysics,* **93**(3–4), 185–199.

Kanamori, H. & Anderson, D.L., 1975. Theoretical basis of some empirical relations in seismology, *Bull. seism. Soc. Am.,* **65**(5), 1073–1095.

Kao, H., 1998. Can great earthquakes occur in the southernmost Ryukyu Arc-Taiwan region?, *Diqiu Kexue Jikan = TAO, Terrestrial, Atmospheric and Oceanic Sciences,* **9**(3), 487–508.

Kao, H. & Rau, R.-J., 1999. Detailed structures of the subducted Philippine Sea Plate beneath Northeast Taiwan: a new type of double seismic zone, *J. geophys. Res.,* **104**(B1), 1015–1033.

Kao, H., Shen, S.-s. J. & Ma, K.-F., 1998. Transition from oblique subduction to collision: earthquakes in the southernmost Ryukyu Arc-Taiwan region, *J. geophy. Res.,* **103**(B4), 7211–7229.

Katsumata, M. & Sykes, L.R., 1969. Seismicity and tectonics of the western Pacific: Izu-Mariana-Caroline and Ryukyu-Taiwan regions, *J. geophys. Res.,* **74**(25), 5923–5948.

Kuochen, H., Wu, Y.M., Chang, C.H., Hu, J.C. & Chen, W.S., 2004. Relocation of Eastern Earthquakes and Tectonic implications, *TAO,* **15**(4), 647–666.

Lallemand, S. & Liu, C.-S., 1998. Geodynamic implications of present-day kinematics in the southern Ryukyus, *J. geol. Soc. China,* **41**(4), 551–564.

Lallemand, S.E., Font, Y., Bijwaard, H. & Kao, H., 2001. New insights on 3-D plates interaction near Taiwan from tomography and tectonic implications, *Tectonophysics,* **335**(3–4), 229–253.

Lallemand, S. *et al*. 2010. The southernmost Ryukyu forearc area (East of Taiwan): an atypical highly faulted margin, Western Pacific Geophysics Meeting, AGU 2010, Taipei.

Lee, W.H.K., Wu, F.T. & Wang, S.C., 1978. A catalog of instrumentally determined earthquakes in China (magnitude> or = 6) compiled from various sources, *Bull. seism. Soc. Am.,* **68**(2), 383–398.

Lee, Y.-H., Chen, G.-T., Rau, R.-J. & Ching, K.-E., 2008. Coseismic displacement and tectonic implication of 1951 Longitudinal Valley earthquake sequence, eastern Taiwan, *J. geophys. Res.,* **113**(B04305), doi:10.1029/2007JB005180.

Letouzey, J. & Kimura, M., 1986. The Okinawa Trough: genesis of a back-arc basin developing along a continental margin, *Tectonophysics,* **125**(1–3), 209–230.

Lienkaemper, J.J., 1984. Comparison of two surface-wave magnitude scales: M of Gutenberg and Richter (1954) and M (sub s) of "Preliminary determination of epicenters", *Bull. seism. Soc. Am.,* **74**(6), 2357–2378.

Ma, K.-F. & Lee, M.-F., 1997. Simulation of historical tsunamis in the Taiwan region, *Diqiu Kexue Jikan = TAO, Terrestrial, Atmospheric and Oceanic Sciences,* **8**(1), 13–30.

Malavieille, J. *et al*. 2002. Arc-continent collision in Taiwan: new marine observations and tectonic evolution, *Special Paper – Geol. Soc. Am.,* **358,** 187–211.

Nakamura, S., 1922. On the destructive earthquakes in Formosa on the 2nd. and 15th. of September, 1922., *Seismol. Bull., Central Meteorol. Obser.,* **1,** 60–69.

Nakamura, M., 2004. Crustal deformation in the central and southern Ryukyu Arc estimated from GPS data, *Earth planet. Sci. Lett.,* **217**(3–4), 389–398.

Nakamura, M., 2009. Aseismic crustal movement in southern Ryukyu trench, southwest Japan, *Geophys. Res. Lett.,* **36**(L20312), 5, doi:10.1029/2009GL040357.

Ng, S.M., Angelier, J. & Chang, C.-P., 2009, Earthquake cycle in western Taiwan: insights from historical seismicity, *Geophys. J. Int.,* **178**(2), 753–774.

Omori, F., 1902. A horizontal Pendulum Tromometer, *Publications of the Earthquake Investigation Committe in Foreign Language,* **12,** 1–7.

Omori, F., 1907. On the estimation of the time of occurrence at the origin of a distant earthquake from the duration of the first preliminary tremor observed at any place, *Imp. earthq. Invest. Com, B,* **1,** 1–4.

Omori, F., 1920. On the relation etween the duration of the preliminary tremor and the epicentral distance for near earthquakes, *Imp. earthq. Invest. Com, B,* **IX**(2), 33–39.

Pacheco, J.F. & Sykes, L.R., 1992. Seismic moment catalog of large shallow earthquakes, 1900 to 1989, *Bull. seism. Soc. Am.,* **82**(3), 1306–1349.

Pezzopane, S.K. & Wesnousky, S.G., 1989. Large earthquakes and crustal deformation near Taiwan, *J. geophys. Res.,* **94**(B6), 7250–7264.

Scholz, C.H., 1990. The mechanics of earthquakes and faulting, Cambridge Univ. Press, New York, NY.

Scholz, C.H., 1998. Earthquakes and friction laws, *Nature* **391**(6662), 37–42.

Shin, T.C., 1993. The calculation of local magnitude from the simulated Wood-Anderson seismograms of the short-period seismograms in the Taiwan area., *Terres. atmos. Oceanic Sci.,* **4**(2), 155–170.

Shin, T.-C. & Teng, T.-l., 2001. An overview of the 1999 Chi-Chi, Taiwan earthquake, *Bull. seism. Soc. Am.,* **91**(5), 895–913.

Shyu, J.B.H., Sieh, K., Chen, Y.-G. & Liu, C.-S., 2005. Neotectonic architecture of Taiwan and its implications for future large earthquakes, *J. geophys. Res.,* **110**(B08402), 33, doi:10.1029/2004JB003251.

Sibuet, J.C. *et al.*1986. Tectonic evolution and volcanism of Okinawa Trough, *Circum-Pacific Energy and Mineral Resource Conference,* Singapore, Vol. 70, p. 934.

Sibuet, J.-C. & Hsu, S.-K. 2004. How was Taiwan created?, *Tectonophysics,* **379**(1–4), 159–181.

Tsai, Y.-B., 1986. Seismotectonics of Taiwan, *Chung Kuo Ti Ch'ih Hsueh Hui Chuan Kan = Memoir of the Geological Society of China,* **7,** 353–367.

Tsai, Y.-B. & Wu, H.-H., 1997. A study on the errors in locating earthquakes due to the geometry of the Taiwan seismic network, *Diqiu Kexue Jikan = TAO, Terrestrial, Atmospheric and Oceanic Sciences,* **8**(3), 355–370.

Tsai, Y.B., Teng, T.L., Hsiung, Y.M. & Lo, C.M., 1973. *New Seismic Data of Taiwan Region,* Annual Report of the Institute of Physics, Taipei, Academia Sinica.

Tsang, Y.-B., Teng, T.-L., Chiu, J.-M. & Liu, H.-L., 1977. Tectonic implications of the seismicity in the Taiwan region, *Mem. Geol. Soc. China,* **2**, 13–42.

Vanek, J., Zatopek, A., Karnik, V., Kondoskaya, N.V., Riznichenko, Y.V., Sevarensky, E.F. , Solovev, S.L. & Shebalin, N.V., 1962. Standardization of magnitude scale. *Izv. Acad. Sci. G. Ser. USSR,* **2,** 108–111.

Wang, J.-H., 1992. Magnitude scales and their relations for Taiwan earthquakes: a review, *DiqiuKexue Jikan = TAO, Terrestrial, Atmospheric and Oceanic Sciences,* **3**(4), 449–468.

Wang, J.-H., 1998. Studies of earthquake seismology in Taiwan during the 1897–1996 period, *J. geol. Soc. China,* **41,** 291–335.

Wang, T.K., 2005. Inverse-ray imaging from triangulation of zero-offset reflection times, *Geophys. J. Int.,* **163**(2), 599–610.

Wang, J.H. & Chiang, S.T., 1987. MD-mb and MD-MS relationships for Taiwan earthquakes, *Proc. Geol. Soc. China,* **30,** 118–124.

Wang, J.-H. & Kuo, H.-C., 1995. A catalogue of M > = 7 Taiwan earthquakes (1900–1994), *J. geol. Soc. China,* **38**(2), 95–106.

Wang, J.-H. & Ou, S.-S., 1998. On scaling of earthquake faults, *Bull. seism. Soc. Am.,* **88**(3), 758–766.

Wang, C.-Y. & Shin, T.-C., 1998. Illustrating 100 years of Taiwan seismicity, *Diqiu Kexue Jikan = TAO, Terrestrial, Atmospheric and Oceanic Sciences,* **9**(4), 589–614.

Wang, T.K., McIntosh, K., Nakamura, Y., Liu, C.-S. & Chen, H.-W., 2001. Velocity-interface structure of the southwestern Ryukyu subduction zone from EW9509–1 OBS/MCS data, *Marine geophys. Res.,* **22**(4), 265–287.

Wang, T.K., Lin, S.-F., Liu, C.-S. & Wang, C.-S., 2004. Crustal structure of southernmost Ryuktyu subduction zone: OBS, MCS and gravity modelling, *Geophys. J. Int.,* **157**(1), 147–163.

Wells, D.L. & Coppersmith, K.J., 1994. New empirical relationships among magnitude, rupture length, rupture width, rupture area, and surface displacement, *Bull. seism. Soc. Am.,* **84**(4), 974–1002.

Wood, H.O., 1914. Concerning the perceptibility of weak earthquakes and their dynamical measurement, *Bull. seism. Soc. Am.,* **4,** 29–38.

Wu, F.T., 1970. Focal mechanisms and tectonics in the vicinity of Taiwan, *Bull. seism. Soc. Am.,* **60**(6), 2045–2056.

Wu, F.T., 1978. *Recent Tectonics of Taiwan,* Sci. Counc. Jpn., Tokyo, Japan (JPN).

Wu, Y.-M., Chang, C.-H., Zhao, L., Teng, T.-L. & Nakamura, M., 2008. A comprehensive relocation of earthquakes in Taiwan from 1991 to 2005, *Bull. seism. Soc. Am.,* **98**(3), 1471–1481.

Wu, Y.-M., Zhao, L. , Chang, C.-H. & Hsu, Y.-J., 2008. Focal-mechanism determination in Taiwan by genetic algorithm, *Bull. seism. Soc. Am.,* **98**(2), 651–661.

Wu, F.T., Liang, W.-T., Lee, J.-C., Benz, H. & Villasenor, A., 2009. A model for the termination of the Ryukyu subduction zone against Taiwan: a junction of collision, subduction/separation, and subduction boundaries, *J. geophys. Res.,* **114**(B07404), 16, doi:10.1029/2008JB005950.

Yeh, Y.-T., Cheng, S.-N., Shin, T.C. & Ho, M.Y., 1995. Assessment of earthquake location and magnitude for several Taiwan catalogs (III), *Central Weather Bureau Technical Report. CWB. Taipei, CWB*. **11,** 243–264.

Yu, S.-B., Chen, H.-Y. & Kuo, L.-C., 1997. Velocity field of GPS stations in the Taiwan area, *Tectonophysics,* **274**(1–3), 41–59.

Zeiler, C. & Velasco, A.A., 2009. Seismogram picking error from analyst review (SPEAR); single-analyst and institution analysis, *Bull. seism. Soc. Am.,* **99**(5), 2759–2770.

Zhang, D.H., Yip, T.L. & Ng, C.-O., 2009. Predicting tsunami arrivals: Estimates and policy implications, *Marine Policy,* **33,** 643–650, doi:10.1016/j.marpol.2008.12.011.

SUPPORTING INFORMATION

Additional Supporting Information may be found in the online version of this article:

Supplement. This Supplement is divided in to four parts. The first one gives all magnitudes of the 1920 earthquake found in the literature and all regression graphs used for magnitude conversion (Table S1 and Fig. S1). The second part provides figures, which show the 1920 analogue-quake determination (Figs S3 and S4). The third part provides documents about archives of the 1920 earthquakes (Fig. S2). The last part provides a tsunami traveltimes map (Fig. S5). Additional references are given at the end. A catalogue with homogenized moment magnitudes higher than 5.0 is also available in the Supporting Information online.

Please note: Wiley-Blackwell are not responsible for the content or functionality of any supporting materials supplied by the authors. Any queries (other than missing material) should be directed to the corresponding author for the article.